Document made available under the Patent Cooperation Treaty (PCT)

International application number: PCT/IL05/000133

International filing date: 03 February 2005 (03.02.2005)

Document type: Certified copy of priority document

Document details: Country/Office: US
Number: 60/554,913
Filing date: 22 March 2004 (22.03.2004)

Date of receipt at the International Bureau: 31 March 2005 (31.03.2005)

Remark: Priority document submitted or transmitted to the International Bureau in compliance with Rule 17.1(a) or (b)

PCT/IL 2005 / 000133
21 MAR 2005

PA 1289982

THE UNITED STATES OF AMERICA

TO ALL TO WHOM THESE PRESENTS SHALL COME:

UNITED STATES DEPARTMENT OF COMMERCE

United States Patent and Trademark Office

March 03, 2005

THIS IS TO CERTIFY THAT ANNEXED HERETO IS A TRUE COPY FROM THE RECORDS OF THE UNITED STATES PATENT AND TRADEMARK OFFICE OF THOSE PAPERS OF THE BELOW IDENTIFIED PATENT APPLICATION THAT MET THE REQUIREMENTS TO BE GRANTED A FILING DATE UNDER 35 USC 111.

APPLICATION NUMBER: *60/554,913*

FILING DATE: *March 22, 2004*

By Authority of the
COMMISSIONER OF PATENTS AND TRADEMARKS

T Lawrence

T. LAWRENCE
Certifying Officer

13281 U.S.PTO

22856 U.S.PTO 60/554913 032204

U.S. PATENT AND TRADEMARK OFFICE
PROVISIONAL APPLICATION FOR PATENT COVER SHEET

This is a request for filing a PROVISIONAL APPLICATION FOR PATENT under 37 C.F.R. §1.53(b)(2)

Atty. Docket: BANIN5

INVENTOR(S)/APPLICANT(S)

LAST NAME	FIRST NAME	MI	RESIDENCE (CITY AND EITHER STATE OR FOREIGN COUNTRY)
BANIN	Uri		Mevasseret Zion, Israel
MOKARI	Taleb		Jerusalem, Israel

[ ] Additional inventors are being named on separately numbered sheets attached hereto

TITLE OF THE INVENTION (280 characters max)

SELECTIVE GROWTH OF METAL TIPS ONTO SEMICONDUCTOR QUANTUM RODS AND TETRAPODS

CORRESPONDENCE ADDRESS

Direct all correspondence to the address associated with **Customer Number 001444**, which is presently:

BROWDY AND NEIMARK, P.L.L.C.
624 Ninth Street, N.W., Suite 300
Washington, D.C. 20001-5303

ENCLOSED APPLICATION PARTS (check all that apply)

[X]	Specification	Number of Pages	13	[X]	Applicant claims small entity status. See 37 C.F.R. §1.27
[X]	Drawing(s)	Number of Sheets	7	[ ]	Other (specify)

METHOD OF PAYMENT (check one)

[X] Credit Card Payment Form PTO-2038 is enclosed to cover the Provisional filing fee of

[ ]$160 large entity [X] $80 small entity

[X] The Commissioner is hereby authorized to charge filing fees and credit Deposit Account Number 02-4035

The invention was made by an agency of the United Stated Government or under a contract with an agency of the United States Government.

[X] No [ ] Yes, the name of the U.S. Government agency and the Government contract number are:

Respectfully submitted,

BROWDY AND NEIMARK, P.L.L.C.

By: Sherdian Neimark
Registration No.: 20,520

Date: March 22, 2004

SN:gsk

Selective Growth of Metal Tips Onto Semiconductor Quantum Rods and Tetrapods

ABSTRACT

Anisotropic selective growth of gold tips onto semiconductor (CdSe) nanorods and tetrapods is carried out by a simple reaction and characterized. The size of the Au tips can be controlled by the concentration of the starting materials. The new nanostructures show significantly modified optical properties as compared to the original rods including broadened and red shifted absorption, and strongly quenched photoluminescence, manifesting the strong coupling between the Au and semiconductor parts. Such gold-tipped nanostructures provide natural contact points for electrical devices and for self-assembly, and can solve the difficult problem of contacting colloidal nanorods and tetrapods to the external world.

Anisotropic growth of nanomaterials has led to the development of complex and diverse nano-structures such as rods [1,2], tetrapods [3], prisms [4], cubes [5], and additional shapes [6,7]. These architectures display new properties and enrich the selection of nano-building blocks for electrical, optical and sensorial device construction. Even greater complexity and new function is introduced into the nanostructure by anisotropic growth with compositional variations. This has been elegantly realized by growing semiconductor heterostructures such as p-n junctions and material junctions in nanowires [8, 9], and in the case of colloidal nanocrystals, in growth of a dot-rod of two different semiconductors [10] and in complex branched growth. In these examples, anisotropic growth was performed with the same material type (semiconductor). Here we report the selective anisotropic growth of two different material systems, a metal onto a semiconductor. We developed a method for the selective growth of gold dots onto the tips of colloidal semiconductor nanorods and tetrapods. This combination provides new functionalities to the nanostructures, the most important of which is the formation of anchor points for directed self assembly presenting an important path for wiring them onto electrical circuitry.

This advancement bears direct relevance for addressing the problem of contact reproducibility and contact resistance that has hindered the study of conductance in nanostructures. Only recently there have been encouraging reports for good connectivity for micron-long quasi-one-dimensional structures such as nanotubes and nanowires [11,12,13]. However, wiring of the significantly shorter colloidal semiconductor rods and tetrapods studied here, with arm lengths of less then 100 nm, is a long standing open issue. The use of bifunctional organic ligands, primarily dithiols, as contacting ligands that has been employed for STM studies [14] and also in transport measurements [15], creates a tunneling barrier and often transport is dominated by the

contact resistances. The employment of DNA based assembly for creating functional circuitry [16,17] also requires selective anchor points for the directed assembly of nanostructures [18]. The selective tip growth of metal contacts as developed here, addresses this key challenge by providing the route to an effective wiring scheme for soluble and chemically processable colloidal semiconductor nanocrystals with rod [1,2], tetrapod [3] or other branched shapes [19]. This would allow to fully realize the potential of miniaturization of devices using such nano-building blocks, while employing the powerful principles of self-assembly to connect them to electrodes or to less conventional DNA circuitry and hence to the 'outside' world.

Our method for selective growth of contacts entails dissolving $AuCl_3$ in toluene by use of dodecyldimethylamonium bromide (DDAB) and dodecylamine, and mixing this solution with a toluene solution of colloidal grown nanorods or tetrapods. The method is exemplified here for the prototypical CdSe nanocrystal system that is highly developed synthetically and widely studied for its size and shape dependent properties [1,20], and is obviously applicable to other semiconductor nanocrystals and potentially to other metals.

CdSe rods and tetrapods of different dimensions (see below), were prepared as described elsewhere, by high temperature pyrolisys of suitable precursors, in a coordinating solvent containing a mixture of trioctylphosphineoxide (TOPO), and of phosphonic acids [1,19,21]. In a typical Au growth reaction, a gold solution was prepared containing 12 mg $AuCl_3$ (0.04mmol), 40 mg of DDAB (0.08mmol) and 70 mg (0.37mmol) of dodecylamine in 3 ml of toluene and sonnicated for 5 minutes at room temperature. The solution changed color from dark orange to light yellow. 20 mg of CdSe quantum rods of the required dimensions were dissolved in 4 ml toluene in a three neck flask under argon. The gold solution was added drop-wise over a period of three

minutes. During the addition, carried out at room temperature, the color gradually changed to dark brown. Following the reaction, the QR's were precipitated by addition of methanol and separated by centrifugation. The purified product could then be redissolved in toluene for further studies.

Fig. 1 presents transmission electron microscopy (TEM) images showing growth of Au onto CdSe quantum rods of dimensions 29x4 nm (length x diameter). Frame A shows the rods before Au growth, while in frames B-D, the gold growth procedure was performed as described above adding gradually larger amounts of Au precursors (see table 1 for details). In frames B-D, selective Au growth onto the rod tips is clearly identified as the appearance of points with enhanced contrast afforded by the higher electron density of the Au compared with CdSe. The rods now appear as 'nano-dumbbells'. Moreover, by controlling the amount of initial Au precursor, it is possible to control the size of the Au tips on the nano-dumbbell edges, from ~2.2 nm in Fig. 1B, to ~2.9 nm in Fig. 1C, to ~4.0 nm in Fig. 1D as summarized in table 1. The procedure clearly leads to the growth of natural contact points on the tips of the rods.

An additional observation from the analysis of ~200 particles per sample is that the overall rod length becomes shorter upon Au growth, and there is also a decrease in the average diameter of the rods, (table 1 and see supplementary Fig. S1 for the complete sizing histograms). Control experiments with the DDAB and dodecylamine without $AuCl_3$ were carried out and also in that case the average rod dimensions decreased (see supplementary table S2). Hence, reduction of rod size is related to dissolution of rods in the presence of DDAB and not to the Au growth.

To verify the material content and structure of the gold on the rod tips we employed several structural and chemical characterization methods as can be seen in Fig. 2. Fig. 2A shows EDS analysis of a micron area of rods after growth and the appearance of Au

in the goldenized and purified rod sample is clear. The powder Xray-diffraction pattern for the 29x4 nm rod sample comparing the rods before and after gold growth is shown in Fig. 2B,. The appearance of the Au (111), (200) and (220) peaks following Au growth is evident, demonstrating crystalline Au is formed on the tips.

Further evidence for Au growth onto single rods, is provided by HRTEM (high resolution TEM) studies of the nano-dumbbells. Fig. 2C shows a HRTEM image of a single rod after gold treatment. The lattice image for the rod part composed of CdSe corresponds to growth of rods along the CdSe <001> axis, consistent with the earlier studies [1,3,21]. The Au is discerned once again as the region at the edge with enhanced contrast and the gold lattice is also shown in Fig. 2D. It is difficult, because of the significant different contrast of the CdSe versus Au, and due to orientation of the rod relative to the electron beam, to observe clearly both lattice images simultaneously, but in different imaging conditions we could verify the presence of the CdSe lattice in the center as seen in Fig. 2C, and the Au lattice in the edges as seen in Fig. 2D. The detailed interface of the Au-CdSe is difficult to study. Our analysis on ~15 rods shows different relative angles for the Au and CdSe lattice, implying that the growth can take place in different forms. However, it is important to note that at the Au-CdSe interface, we can expect Au-Se bonds, analogous to the known AuSe material [22]. This means that the interface is formed with covalent chemical bonds between the metal and the semiconductor and hence can be expected to provide good electrical connectivity.

The method for selective Au growth could be easily expanded and applied to rods of arbitrary dimensions, and to tetrapods, as well as to growth of other metals and to rods made of various semiconductor materials.

Fig. 3 shows TEM images for three rod samples of dimensions 12x4 nm (Fig. 3A, B), 29x4 nm (Fig. 3C, D), and 60x6 nm (Fig. 3E, F), before and after Au treatment. The

presence of the high-contrast tips on the treated rods, forming nano-dumbbells, is evident in all cases. Highly selective tip growth is discerned and demonstrated for three rod sizes and could easily be applied to arbitrary rod sizes. In addition the method was applied to a CdSe tetrapod sample, as can be seen in Fig. 2G showing several tetrapods, and in Fig. 2H showing an enlargement of one tetrapod, following the Au growth process. In this case, the growth occurs selectively on all the tips of the tetrapods leading a tetrahedral arrangement for the Au tips, and once again providing the natural contact points for this unique structure, for further self-assembly and for electrical connections.

The metalized structures (in the case of Au growth we may term the formed structures "goldenized structures") are expected to exhibit new and different electronic, electrical and optical properties as compared to the original rods, due to the strong effect of the metal on the semiconductor properties. We have grown metal tips by the method described above also onto CdSe/ZnS core/shell nanorods (29x4 nm rods with 2 monolayer ZnS shell) with initial emission quantum yield of 2%. Treatment of these rods with DDAB and dodecylamine without Au led to an increased quantum yield of 4%, likely because of the effect of the excess amine. Several Au sizes were grown from ~2 nm to 4.5 nm Au at the tips of the rods. Absorption and photoluminescence (PL) measurements were carried out to study the effect of Au growth on the rod optical properties as shown Fig. 4. Absorption spectra (Fig. 4A) for the small Au tips on the rods still shows the excitonic structure but with increased absorbance in the visible and the appearance of a tail to the red of the particle gap. Upon increased Au size, the features of the absorption of the rods are washed out and the tail to the red becomes more prominent. The spectra should contain in principle contributions from the semiconductor part and the plasmon resonance associated with the Au tips. However,

we emphasize that attempts to add spectra of the rod template and Au nanocrystals did not reproduce the observed absorption and we conclude that the spectra are not a simple sum of both components. Instead, these results reflect the modified electronic structure of the Au-rod nano-dumbbell system. The strong mixing of the semiconductor and metal electronic states leads to modified density of states exhibiting broadened levels and a reduced band-gap.

The significant coupling of the Au is also observed for the PL (Fig. 4B) that undergoes considerable quenching with increased Au ball size, by a factor of ~100 initially for the smaller Au balls (~2 nm), and gradually down to a factor of ~500 for the large Au balls (~4.5 nm). Quenching of the emission by the metal edges is expected via the new non-radiative pathways created by the proximity of metals, likely leading to electron transfer to the Au. This behavior resembles the super-quenching effect by highly efficient energy transfer from conjugated polymers to gold nanoparticles [23]. Moreover, a systematic dependence of quenching on Au size is seen as shown in the Stern-Volmer type plot (inset of Fig. 4B), resembling the observation in the Au-polymer case [24]. Both absorption and emission spectra exemplify the significant effect of the Au on the semiconductor rod properties in this new system, further proving the strong bonding of the Au to the CdSe rod.

The selective tip growth of Au onto the rods and tetrapods not only provides important developments for enabling electrical connectivity and new paths for self-assembly for such nanostructures. It is also an interesting and novel chemical reaction route with clear selectivity and anisotropic character. The reaction mechanism for the gold growth entails a reduction of Au. Examining by TEM the Au solution with DDAB and dodecylamine, we already find formation of Au particles (supplementary Fig. S3). This is consistent with earlier reports on formation of Au particles with amine

precursors [25], and also for Ag nanoparticle formation in mild conditions [26]. The further role of dodecylamine is revealed from experiments carried out without amine. In this case, considerable aggregation of the CdSe rods was seen (supplementary Fig. S4). Dodecylamine is known to stabilize the rods and prevent aggregation [27]. Additionally, without the amine, growth of Au on rods was not apparent initially and only after the irradiation under the electron beam of the TEM we could observe some Au growth (supplementary Fig. S4).

The most compelling aspect of the procedure reported here is its specificity leading to selective tip growth. This is assigned to the preferential adsorption of the Au complex onto the rod tips. The tips are more reactive due to the increased surface energy and also possibly due to imperfect passivation of the ligands on these faces, which also leads to preferential growth along the <001> axis of CdSe rods [1,3]. Once Au nucleates on the edge, it is preferential for additional Au to adhere and grow on that seed. This gains support from controlling the extent of Au growth on the rod tips by using increased concentration of Au in the gold solution as was shown in Fig. 1. Moreover, early Au growth as shown in Fig. 1B reveals that in some rods preferential early growth occurs on one tip, in agreement with the surfactant-controlled growth model suggested for CdSe rods [1,19,21]. From the viewpoint of chemical reactivity, the asymmetry in reaction to selectively occur at the tips versus the rest of the nanostructure is fascinating.

It is important to note that in some cases we can identify Au growth on branching and defect points, but at slower rate compared to the distinctive tip growth discussed above. This can be seen in Fig. 3E and 3G, where weak dark Au spots appear also in some positions other then the tips of the long rods and tetrapods. This growth can be controlled by the amounts of Au added to the rods. At such defect points, such as points

where the diameter of the structure changes, there is also increased reactivity due to the imperfect chemical bonding and increased surface energy. This leads to Au adhesion and growth in agreement with the mechanism for tip growth. We emphasize that the tip growth occurs more readily and rapidly then growth on the defects and hence can be controlled to achieve contact points.

The method may easily be expanded to additional semiconductor nanocrystal systems and to additional metals, to tailor the metal tip contacts as desired and the semiconductor element as well. The new nanostructures could reveal new linear and non-linear optical properties related with the highly polarizable metal edges. They are tailored for new schemes of edge-directed self assembly based on the chemically distinct metal points. The metal tips can serve as nucleation sites for further growth of metallic or semiconductor layers. Following attachment to metal electrodes, it is possible to employ rapid thermal annealing at relatively low temperatures to 'fuse' the tips to the electrodes and achieve good electrical contact, while taking advantage of the reduced melting point in small diameter nanocrystals. A straightforward utilization of the Au tips will be in serving as a contact point for wiring them onto conventional electrode circuits or novel self-assembled circuitry.

REERENCES:

1. X. G. Peng, L. Manna, W. D. Yang, J. Wickham, E. Scher, A. Kadavanich and A. P. Alivisatos, *Nature* **404**, 59 (2000).

2 S. H. Kan, T. Mokari, E. Rothenberg and U. Banin, *Nat. Mat.* **2**, 155 (2003).

3. L. Manna, D. J. Milliron, A. Meisel, E. C. Scher, and A. P. Alivisatos, *Nat. Mat.* **2**, 382 (2003).

4. R. Jin, Y. Cao, C. A. Mirkin, K. L. Kelly, G. C. Schatz, J. G. Zheng, *Science* **294**, 1901 (2001).

5. F. Dumestre, B. Chaudret, C. Amiens, P. Renaud, P. Fejes, *Science* **303**, 821 (2004).

6. Z. Y. Tang, N. A. Kotov and M. Giersig, *Science* **297**, 237 (2002).

7. J. Goldberger, R. He, S. Lee, Y. Zhang, H. Yan, H. Choi, P. Yang, *Nature* **422**, 599 (2003).

8. M. S. Gudiksen, L. J. Lauhon, J. Wang, D. Smith, and C. M. Lieber, *Nature* **415**, 617 (2002).

9. Y. Wu, R. Fan, P. Yang, *Nano Lett.* **2**, 83 (2002).

10. D. V. Talapin, R. Koeppe, S. Goltzinger, A. Kornowski, J. M. Lupton, A. L. Rogach, O. Benson, J. Feldmann, and H. Weller, *Nano Lett.* **3**, 1677 (2003).

11. Y. Cui and C. M. Lieber, *Science* **291**, 851 (2001).

12. S. Heinze, J. Tersoff, R. Martel, V. Derycke, J. Appenzeller, and Ph. Avouris, *Phys. Rev. Lett.* **89**, 106801 (2002).

13. A. Javey, J. Guo, Q. Wang, M. Lundstrom and H. Dai, *Nature* **424**, 654 (2003).

14. U. Banin, O. Millo, *Ann. Rev. Phys. Chem.* **54**, 465 (2003).

15. D. L. Klein, R. Roth, A. K. L. Lim, A. P. Alivisatos, & P. L. McEuen, *Nature* **389**, 699 (1997).

16. E. Braun, Y. Eichen, U. Sivan, G. Ben-Yoseph, *Nature* **391** ,775 (1998).

17. H. Yan, S. H. Park, G. Finkelstein, J. H. Reif, T. H. LaBean, *Science* **301**, 1882 (2003).

18. K. Keren, R. S. Berman, E. Buchstab, U. Sivan and E. Braun, *Science* **302**, 1380 (2003).

19. L. Manna, E. C. Scher, and A. P. Alivisatos, *J. Am. Chem. Soc.* **122**, 12700 (2000).

20. C. B. Murray, D. J. Norris, M. G. Bawendi, *J. Am. Chem. Soc.* **115**, 8706 (1993).

21. Z. A. Peng, X. Peng, *J. Am. Chem. Soc.* **123**, 1389 (2001).

22. J. E. Cretier and G. A. Wiegers, *Mat. Res. Bull.* **8**, 1427 (1973).

23. C. Fan, S. Wang, J. W. Hong, G. C. Bazan, K. W. Plaxco, and A. J. Heeger, *PNAS* **100**, 6297 (2003).

24. R. M. Jones, L. Lu, R. Helgeson, T. S. Bergstedt, D. W. McBranch, and D. G. Whitten, *PNAS* **98**, 14769 (2001).

25. S. Gomez, K. Philippot, V. Colliere, B. Chaudret, F. Senocq, and P. Lecante, *Chem. Comm.* 1945 (2000).

26. M. Yamamoto and M. Nakamoto, *J. Mater. Chem.* **13**, 2064 (2003).

27. T. Mokari, U. Banin, *Chem. Mater.* **15**, 3955 (2003).

Table 1: Details for Au growth on 29x4 nm rods as shown in Fig. 1 and average dimensions (full histograms shown in supplementary Fig. S1).

Sample	NC's amount(mg)	HDA amount(mg)	DDAB amount(mg)	$AuCl_3$ amount(mg)	Rods size (L x D) nm	Gold ball size(nm)
1	-	-	-	-	29 x 4 nm	(original rod)
2	10 mg	40mg	25 mg	4mg	25.6 x 3.3 nm	2.22 nm
3	10 mg	90 mg	50 mg	8 mg	23.9 x 3.4 nm	2.9 nm
4	10 mg	160 mg	100 mg	13.5 mg	20.8 x 3.2 nm	4 nm

FIGURE CAPTIONS:

Figure 1: Controlled growth of Au onto the tips of CdSe quantum rods. TEM images are shown for A. Original 29x4 nm rod sample. B, C, D. Rod samples 2, 3 and 4, respectively (table 1) after Au treatment using gradually increased $AuCl_3$ concentrations and showing gradually increased Au tip sizes.

Figure 2: Structural and chemical characterization of CdSe-Au 'nano-dumbbells'. A. Energy dispersive Xray spectroscopy (EDS) spectrum on the goldenized CdSe rod sample. The relative atom percentage of Au:Cd:Se was18%:42%:40%. B. Powder Xray diffraction comparing CdSe rods before (1), and after (2) Au growth. Bulk CdSe and Au peaks are marked. Crystalline Au clearly appears after the growth process. Intensity re-distribution in favor of (002) CdSe peak in the original rods is a result of partial alignment in the deposited rod sample, in which rods grow along <001>. C, D. HRTEM images of a single nano-dumbbell and a nano-dumbbell tip, respectively. The CdSe lattice for the rod in the center, and Au tips at the rod edges, can be identified as marked.

Figure 3: Au growth on tips of various CdSe quantum rods and CdSe tetrapods. A, B. 12x4 nm quantum rods before and after Au growth, respectively. C, D. 29x4 nm quantum rods before and after Au growth, respectively. E, F. 60x6 nm quantum rods before and after Au growth, respectively. G, H. Au growth on CdSe tetrapods showing a general view (G), and higher magnification image for one tetrapod (H).

Figure 4: Optical spectra for CdSe/ZnS core/shell nanorod sample with varied Au tip size compared to the original rod template. A. Absorption spectra where Au tip size is indicated. Spectra are offset vertically for clarity. Inset shows TEM image of the

sample after Au growth (scale bar is 50 nm). B. Photoluminescence spectra where Au tip size is indicated for each trace. Traces were multiplied by 25, 50 and 50 for the 2 nm, 3.2 nm, and 4.5 nm Au tips, respectively, for clarity. Inset shows a plot of relative PL yield for template (Φ_0) over Au-rod (Φ), versus Au ball size. Measurements were performed for rod solutions in a sealed cuvette under Ar using the 454 nm line of an Ar-ion laser with intensity of 100 mW. Fluorescence was collected using identical conditions for all solutions in a right angle configuration with a spectrograph/CCD setup, with 500 ms integration time.

FIGURES

Figure 1 :

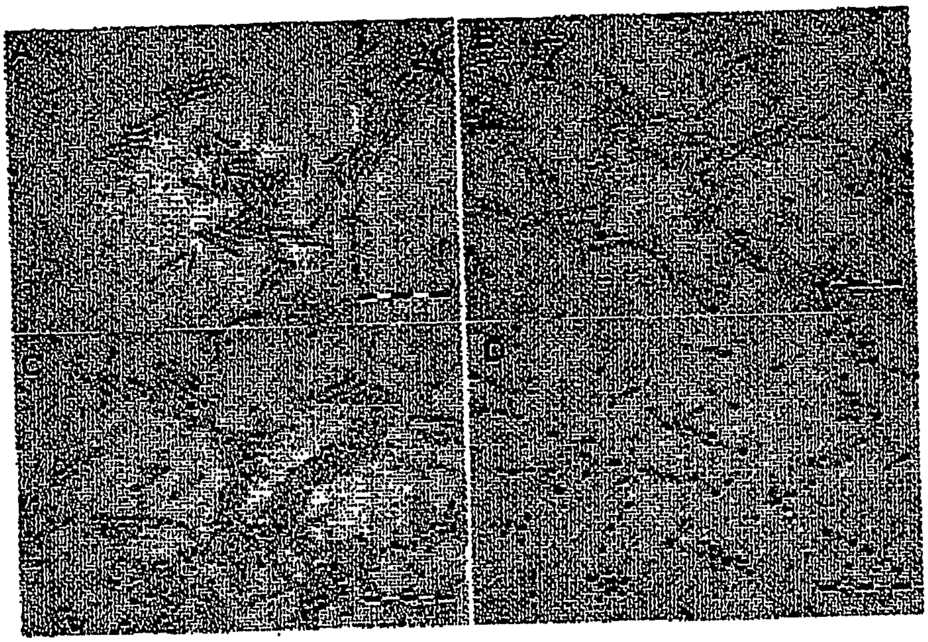

01521996\10-01

Figure 2 :

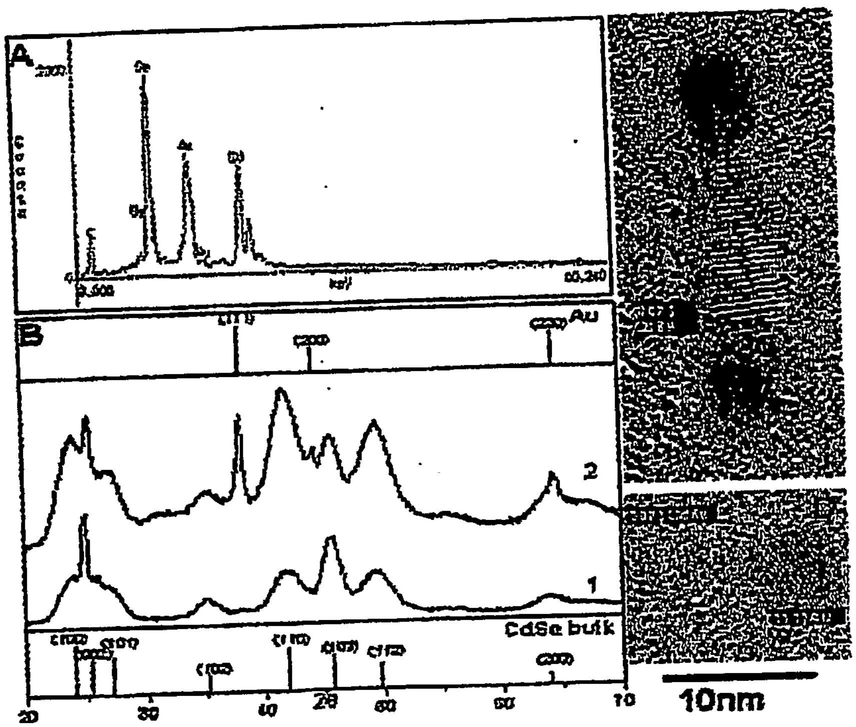

01521996\10-01

Figure 3:

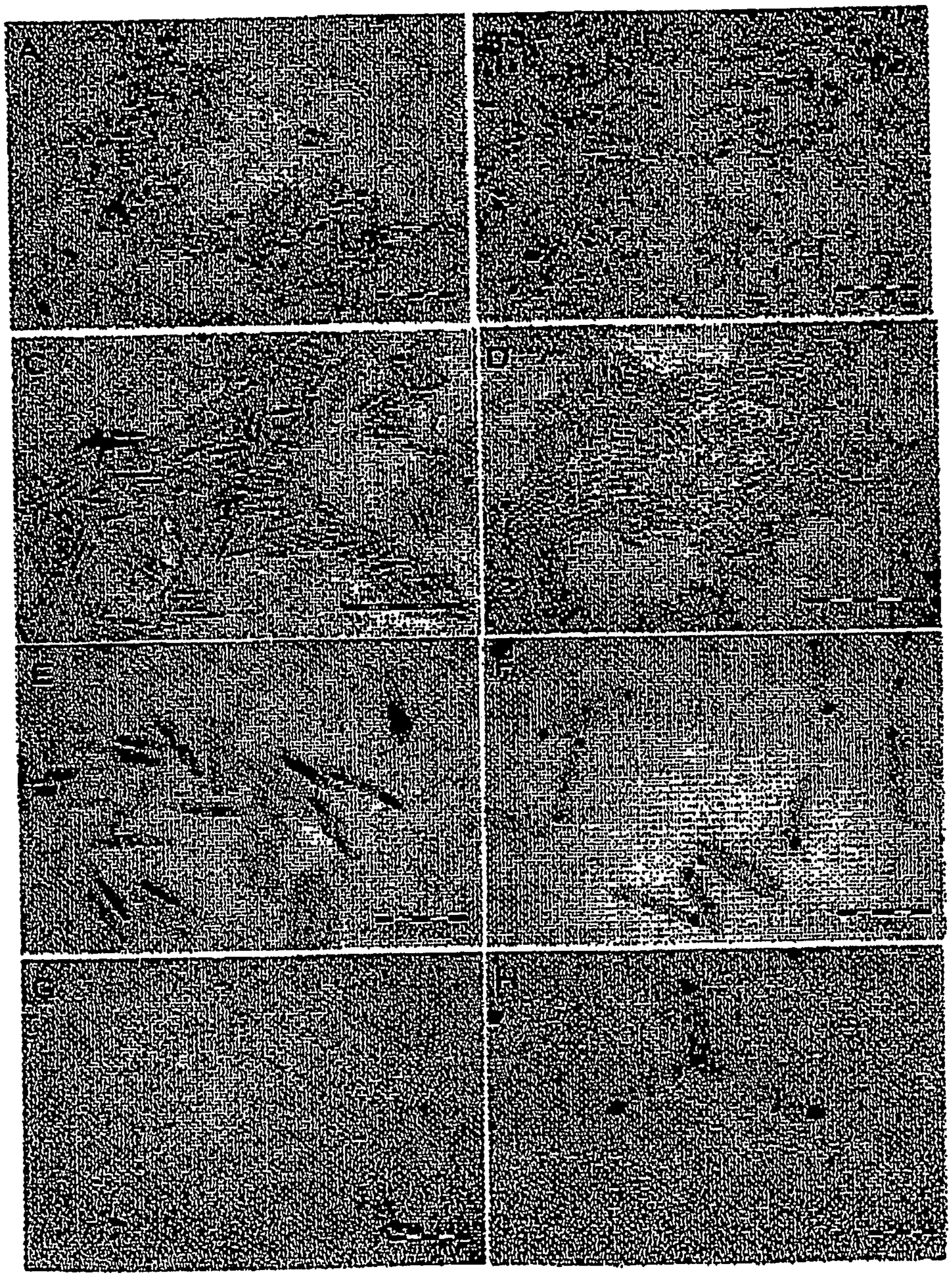

01521996\10-01

Figure 4:

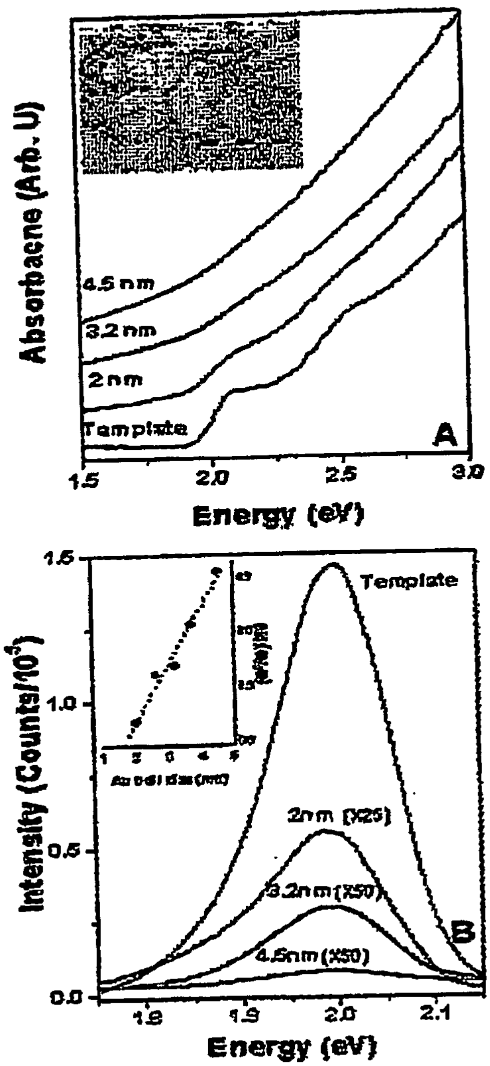

01521996\10-01

SUPPLEMENTARY INFORMATION:

Supplementary figure S1: Sizing histograms for goldenized rods shown in Fig. 1 in the paper for ~200 particles per sample. Histograms for rod diameter (left), length (center) and Au diameter (right) are shown for the four samples: 1. Original 29x4 nm rods, 2. Rods (10 mg) with 4 mg $AuCl_3$, 25 mg DDAB and 40 mg dodecylamine. 3. Rods (10 mg) with 8 mg $AuCl_3$, 50 mg DDAB and 90 mg dodecylamine. 4. Rods (10 mg) with 13.5 mg $AuCl_3$, 100 mg DDAB and 160 mg dodecylamine. The average values are presented in table 1.

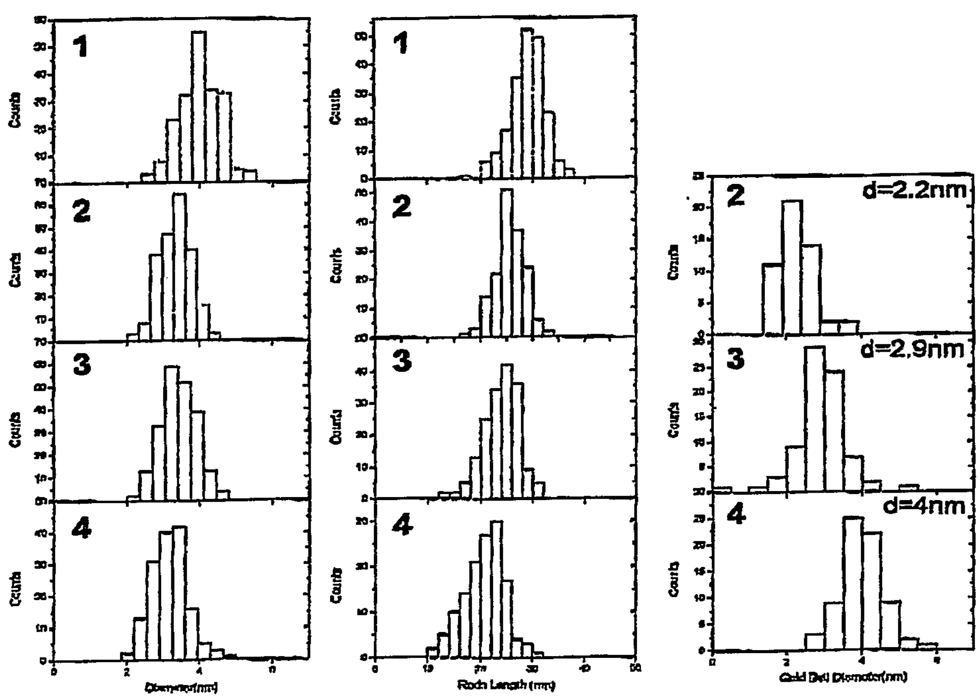

Supplementary table S2: Effect of DDAB and dodecylamine on rods without $AuCl_3$ added. Rod etching by the solution is evident leading to decrease in rod length and diameter. All experiments carried out in 3 ml of toluene.

Sample	NC's amount(mg)	HDA amount(mg)	DDAB amount(mg)	Average rod size (L x D) nm
1	(original rod)	-	-	29 x 4 nm
2	10 mg	70mg	30 mg	26.7 x 3.5 nm
3	10 mg	90 mg	60 mg	25.5 x 3.4 nm
4	10 mg	145 mg	95 mg	24 x 3.2 nm

Supplementary figure S3: TEMs of product from adding $AuCl_3$ with DDAB and amine in toluene. Au particles and aggregates are formed.

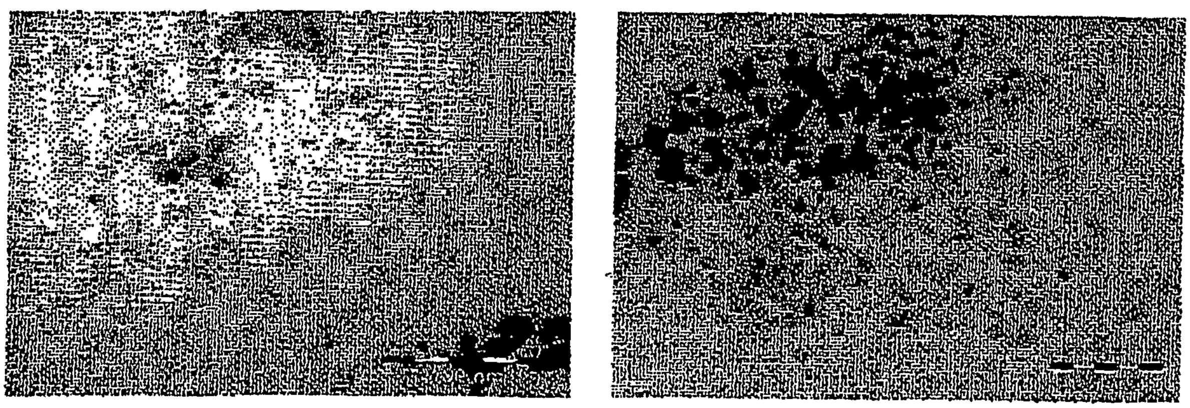

Supplementary figure S4: TEM of product from mixture of rods with $AuCl_3$ and DDAB without dodecylamine. A. before exposure to the TEM electron beam – aggregated rods are seen. B. after exposure to the TEM electron beam – Au patches appear on the rods.